GaN and InN conduction-band states studied by ellipsometry

Munise Rakel,* Christoph Cobet,† and Norbert Esser
ISAS-Institute for Analytical Sciences, Department Berlin, Albert-Einstein-Strasse 9, D-12489 Berlin, Germany

Frank Fuchs and Friedhelm Bechstedt
Institut für Festkörpertheorie und -optik, Friedrich-Schiller-Universität, Max-Wien-Platz 1, D-07743 Jena, Germany

Rüdiger Goldhahn
Institut für Physik, Technische Universität Ilmenau, PF 100565, D-98684 Ilmenau, Germany

Wolf Gero Schmidt
Theoretische Physik, Universität Paderborn, Warburger Strasse 100, D-33095 Paderborn, Germany

William Schaff
Institute for Electrical Engineering, Cornell University, Ithaca, New York 14853, USA
(Received 20 August 2007; revised manuscript received 14 February 2008; published 17 March 2008)

The complex dielectric function (DF) of wurtzite InN and GaN as well as zinc blende GaN was measured by spectroscopic ellipsometry between 14 and 32 eV with synchrotron radiation. In this spectral region, the DF of InN and GaN originates from Ga 3*d* and In 4*d* core level transitions to unoccupied conduction-band states. The Ga 3*d* and In 4*d* electronic states are highly localized and show almost no dispersion. We use these core states as a reference in order to probe the conduction bands. For this purpose, the imaginary part is compared to the density of empty *p*-orbital-like electronic states located around the cation atomic site, as calculated by density-functional theory in the local density approximation. The constant splitting of absorption features in the DF is attributed to the spin-orbit splitting of the *d* states. $\Delta d_{5/2-3/2}$ is found to be 0.82 eV for the In 4*d* and 0.41 eV for the Ga 3*d* level, respectively. On wurtzite samples with the *c* axis in the surface plane, ellipsometry measurements give access to both independent dielectric tensor components $\varepsilon^{\parallel}$ and $\varepsilon^{\perp}$, respectively. The observed anisotropy is induced by a directional dependence of empty *p* states yielding a $p^{\parallel}$-DOS (density states) different to the $p^{\perp}$-DOS.

DOI: 10.1103/PhysRevB.77.115120 PACS number(s): 71.20.−b, 71.55.Eq, 71.15.Mb, 78.20.−e

I. INTRODUCTION

The investigation of the optical properties of materials in the infrared to ultraviolet spectral range is a quite common approach to gain information about vibronic and electronic excitations. For instance, light emission, absorption, and reflection spectroscopy techniques are usually employed to study the electronic band structure and excitonic features of semiconductors. Spectroscopic ellipsometry (SE) is a reference-free reflection method to determine the complex dielectric function of solids in a wide range of photon energies. By analyzing the change of polarization of linear polarized light reflected under an angle of incidence near the Brewster angle, two independent quantities are obtained in a single measurement. These can be converted into real and imaginary parts of the dielectric function or dispersion and absorption coefficients in a straightforward manner. Moreover, linear polarized light is very useful for studying anisotropic materials.

In recent years, SE has been intensively used to study the optical properties of III-nitrides from the near infrared to the ultraviolet up to 10 eV. In this spectral region, the dielectric function (DF) provides valuable information about the electronic band structure since the imaginary part of the DF is closely related to the joint density of electronic states. Consequently, features in the DF show up at interband critical points, i.e., the fundamental and higher order band gaps. Furthermore, the determination of the DF or optical coefficients *n* and *k* is essential for the layout of optoelectronic devices. The technological interest in III-nitrides is immense because optoelectronic devices based on alloys of In-, Ga-, and Al-nitride can cover a very broad spectral region from the near-infrared (fundamental band gap of InN: 0.68 eV) up to the deep ultraviolet (fundamental band gap of AlN: 6.21 eV). Nevertheless, basic understanding of the electronic properties such as the electronic band structure is still not satisfactory. For instance, the interaction of the In 4*d* and Ga 3*d* core electrons with the valence states complicate theoretical descriptions, and the value of the fundamental band gap of InN is still under discussion.

The thermodynamically stable polytype of III-nitrides is the hexagonal wurtzite structure, which is uniaxially anisotropic in contrast to the metastable cubic zinc blende structure. The majority of nitride samples studied so far are wurtzite [0001] films with the *c* axis perpendicular to the surface. Accordingly, the DF was mostly determined for electric field components perpendicular to the [0001] *c* axis ($\varepsilon^{\perp}$). The parallel component $\varepsilon^{\parallel}$ was measured so far only in a few experiments, for example, by SE on $[1\bar{1}00]$ and $[11\bar{2}0]$ films.[1–3]

In the present work, we address the band structure of GaN and InN by determining the DF in the vuv spectral range and comparing the experimental results with *ab initio* DFT-LDA

 ©2008 The American Physical Society

calculations. Above 15 (18) eV, the optical properties of the nitrides are governed by excitations of the In $4d$(Ga $3d$) core levels to empty conduction-band states. This part of the dielectric function will be used here in order to study the conduction-band density of states.[4] Core level excitations are usually investigated with electron energy loss spectroscopy or x-ray absorption spectroscopy. However, we will use spectroscopic ellipsometry, which provides superior spectral resolution and a more direct access to the optical functions. Approximations in subsequent Kramers–Kronig analysis, for instance, are avoided.

The electronic structures of InN and GaN are closely related. The metal atoms in both materials provide completely filled d shells (In $4d$ and Ga $3d$), which are accessible in our measurements. These electronic states have a binding energy of about 16–18 eV below the valence band maximum.[5,6] Several *ab initio* band structure calculations based, e.g., on density-functional theory (DFT) have been published for InN and GaN. In some of these studies,[7,8] the d electrons are frozen into the core, while others explicitly include them in the valence shell where they can interact (hybridize) with the N $2s$ valence states in near resonance.[9,10] Discrepancies in the publications exist especially for InN concerning the sd coupling, the pd repulsion, and quasiparticle corrections.[11] Both the sd coupling and the pd repulsion are supposed to be responsible for the narrow band gap of InN. The N $2s$–In $4d$(Ga $3d$) relation was also probed by x-ray photoelectron spectroscopy (XPS) where the N $2s$ band appears as a small shoulder in the In $4d$(Ga $3d$) spectra.[5,12–14] Piper *et al.* determined the In $4d_{5/2}$ level (in the In-N bonds) 16.0 eV below the valence band maximum together with a very small N $2s$ band contribution at about 13.5 eV binding energy.[5] However, all these results show a large dominance of the cation d levels within the deep valence band density of states (VB-DOS). Due to the strong localization around the III-metal cores, these d states are almost concentrated in a nondispersive band and occur as a sharp peak in the calculated as well as in the experimental VB-DOS.[5,10,15,16] It is therefore possible to use them as a reference energy for probing the conduction-band (CB) characteristics in respective absorption or reflection based methods.

II. EXPERIMENT

The measurements were performed with a custom made rotating analyzer ellipsometer[17,18] at the "Berliner Elektronenspeicherring-Gesellschaft für Synchrotronstrahlung" (BESSY II) using the toroidal grating monochromator (TGM-4) beamline. All optical components as well as the sample are mounted in an ultrahigh vacuum (UHV) chamber. The base pressure in the chamber was kept at 5×10^{-10} mbar. The UHV environment allows us to heat the samples for cleaning and to perform low-temperature measurements without surface contamination. For the ellipsometric measurements, we use an angle of incidence of 45°, which nearly fits the Brewster angle in the investigated spectral range. Since no birefringent transparent materials transmit light above 10 eV, the incoming monochromatized synchrotron radiation was linearly polarized and finally analyzed by triple gold reflection polarizers. The high energy limit of our measurements is determined by the reflectivity of the samples at 45° angle of incidence. Above the plasma frequency, the reflectivity decreases rapidly and under-run a critical value above 32 and 30 eV for GaN and InN, respectively.

GaN was studied in both crystal modifications, in zinc blende and wurtzite structures. The best results were achieved with a high quality commercial c-plane wurtzite GaN[0001] sample grown by metal-organic vapor phase epitaxy on Al_2O_3[0001] (Cree Research Inc.). The root mean square (rms) surface roughness is less than 0.6 nm determined by atomic force microscopy (AFM). This GaN layer is 1780 nm thick and has a rocking-curve full width half maximum of 0.11° observed by x-ray diffraction (XRD). However, due to the [0001] crystal orientation, the determination of dielectric properties is limited to the ordinary DF $\varepsilon^{\perp}$. Between 3 and 10 eV, this dielectric tensor component was already measured on the same sample.[19] However, in order to study both dielectric tensor components, samples are required with off-normal c-axis orientation. We used epitaxial M-plane GaN[$1\bar{1}00$] layers on γ-$LiAlO_3$[100] substrates grown by molecular beam epitaxy (MBE) in the Paul Drude Institute, Berlin.[20] The layer thickness is about 600 nm and the rms surface roughness is 3 nm. A thermal mismatch of the GaN($1\bar{1}00$) film and the γ-$LiAlO_3$ substrate leads to a compressive in plane strain of about −0.3% and dilation of 0.3% parallel to the growth direction.[21] The orientation of the c axis in the surface plane was determined by reflectance anisotropy spectroscopy with 90° angle of incidence. Subsequently, ellipsometric measurements were performed in the two high symmetry orientations, where the c axis is parallel or perpendicularly oriented to the plane of incidence. With these measurements, we obtain a set of two effective dielectric functions very close to the extraordinary and ordinary DFs $\varepsilon^{\parallel}$ and $\varepsilon^{\perp}$, respectively. The cubic GaN film was grown on a GaAs substrate by MBE in the University of Paderborn.[22] This film was characterized by XRD to have at least 99% cubic phase. The layer thickness is 400 nm and the rms surface roughness was determined to be 5 nm.

The DF of InN was measured on a c-plane InN[0001] film grown by plasma assisted MBE on Al_2O_3[0001] with a layer thickness of 1070 nm. Room temperature Hall measurements yielded an electron concentration of 1.5×10^{18} cm^{-3} and a mobility of 1200 cm^2/V s. AFM revealed a rms surface roughness of 1.2 nm for this sample. The recent success in growing a-plane InN[$11\bar{2}0$] single crystalline films also gave access to the extraordinary DF $\varepsilon^{\parallel}$ of InN. These films were grown by MBE, as described in Ref. 23 The crystal orientation is induced by an r-plane $1\bar{1}02$ sapphire substrate with a GaN buffer layer. The used film has a thickness of 670 nm and the surface roughness was determined to be 6 nm (rms roughness) by AFM. The free carrier concentration in this sample is 6×10^{18} cm^{-3}. Both InN samples were already used to collect ellipsometric data below 10 eV.[24]

The ellipsometric spectra presented in this work are so-called effective dielectric functions $\langle \varepsilon \rangle$, which means that a two-phase model (upper half space, vacuum; lower half

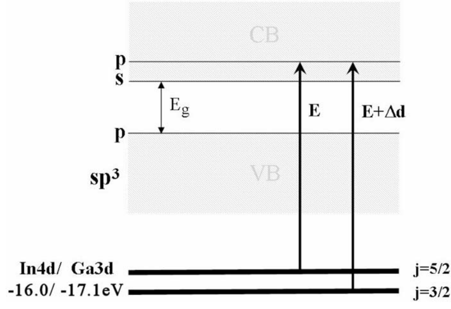

FIG. 1. Simplified scheme of band ordering in InN and GaN. The deep lying d levels of the III-metal atoms are quasidispersionless but split by spin-orbit interaction and crystal field effects. The arrows mark the kind of electronic transitions, which are mainly observed in our ellipsometric measurements.

space, uniaxial anisotropic nitrides) was applied for the calculation of the dielectric function. Hence, we neglect the finite thickness of the nitride layers and, for example, the effect of surface roughness. With a light penetration depth of less than 50 nm, the finite layer thickness (>400 nm), in fact, does not contribute to the measured data. In contrast, surface roughness or unintentional surface contamination should be taken into account in order to extract absolute values for the material constants. In our study, however, we focus our attention on the line shape and peak energies rather than absolute amplitudes. The line shape and the interpretation in terms of involved electronic transitions are not affected by a small surface roughness or contamination layer in the order of 1 nm; they only cause a damping of amplitudes.

III. DIELECTRIC FUNCTION OF *d*-STATE EXCITATIONS

A very simplified scheme of the excitation of In $4d$(Ga $3d$) electrons to unoccupied states is drawn in Fig. 1. Here, we consider the splitting of d states by the relativistic spin-orbit interaction and the hexagonal crystal field. According to the Ehrenreich–Cohen formula,[25–27] the dielectric function can be obtained from a sum over all electric dipole transitions from occupied valence band to empty conduction-band states in the entire Brillouin zone.[28] This summation can also be expressed as a sum of all valence–conduction-band pairs and an integration over all surfaces of a constant energy E_{cv} within these band pairs,[29]

$$\varepsilon[\omega] = 1 + \frac{1}{4\pi^3}\frac{e^2}{\varepsilon_0 m_e^2 \hbar^2}\sum_{c,v}\int_0^\infty dE_{cv}P_{cv}\frac{J[E_{cv}]}{\omega^2} \times\left(\frac{1}{\hbar\omega + E_{cv} + i\Gamma} - \frac{1}{\hbar\omega - E_{cv} + i\Gamma}\right). \quad (1)$$

P_{cv} denotes the dipole transition matrix element in a certain band pair, which is assumed to be k independent. E_{cv} is the energy difference between valence and conduction-band states, while Γ denotes a broadening parameter related, e.g., to the lifetime broadening of excited states.[30] $J[E_{cv}]$ is the so-called joint density of states between valence and conduction bands,

$$J[E_{cv}] = \int_{S_{E_{cv}}} \frac{dS_{\vec{k}}}{|\nabla_{\vec{k}} E_{cv}[\vec{k}]|}, \quad (2)$$

where the integration is performed on the constant $E_{cv}[\vec{k}]$ surface. It was noted already in the Introduction that the strongly localized In $4d$ and Ga $3d$ states are predominantly concentrated in nondispersive bands.[5,10,15,16] This localization is also confirmed in our calculation as shown in Fig. 5. The occupied states under investigation, thus, can be assumed to be k independent and Eq. (2) reduces to

$$J[E_{cv}] = \int_{S_{E_{cv}}} \frac{dS_{\vec{k}}}{|\nabla_{\vec{k}}(E_c[\vec{k}] - E_v)|} = \int_{S_{E_{cv}}} \frac{dS_{\vec{k}}}{|\nabla_{\vec{k}} E_c[\vec{k}]|}, \quad (3)$$

which is the conduction-band density of states (CB-DOS). The contribution to ϵ_2 from either one of the spin-orbit components is proportional to the density of states in the CB divided by ω^2. Final states with s or d symmetry are forbidden due to the dipole selection rules ($P_{cv}=0$). Only the p-like orbitals (conduction bands) contribute to the measured dielectric function. Accordingly, the InN and GaN ellipsometric spectra above 16 eV can be used to explore the site specific density of p-like empty states in a similar manner, as known from x-ray absorption on the N $1s$ core level edge.[31] In other words, specific structures in the dielectric function can be associated with maxima in the density of p-like empty states. This contribution of d-level excitations to the optical properties of GaN above 20 eV was considered already by Lambrecht *et al.* in an earlier work.[13] They conclude that the contributions of the N $2s$ valence bands can be ignored, while the N $2p$ conduction bands cause a small gradually decreasing background.

IV. COMPUTATIONAL METHODS

The *ab initio* calculations have been performed in the framework of DFT as implemented in the Vienna *ab initio* simulation package (VASP).[32] For exchange and correlation, the local density approximation (LDA) together with generalized gradient corrections in the case of GaN was used. The electron-ion interaction was described using the projector augmented wave method.[33] This allows for the accurate treatment of the first-row element nitrogen as well as the Ga $3d$ and In $4d$ states, which were treated as valence states, at modest plane wave cutoffs. The plane wave cutoffs were chosen to be 400 eV for both GaN and InN. To ensure the convergence with respect to the number of k points, $18\times18\times10$ meshes of the Monkhorst–Pack type were used for both materials together with the tetrahedron method[34] for integrations in the Brillouin zone. For InN, the LDA calculation predicts a zero gap semiconductor with a wrong ordering of the $\Gamma_{1,c}$ and the $\Gamma_{6,v}$, $\Gamma_{1,v}$ levels.[11] However, this was found to be irrelevant for the present calculations of the p-symmetric partial DOS of the lower conduction states. The same holds for quasiparticle effects, which were found to preserve the line shape with only minor variations of the peak positions.

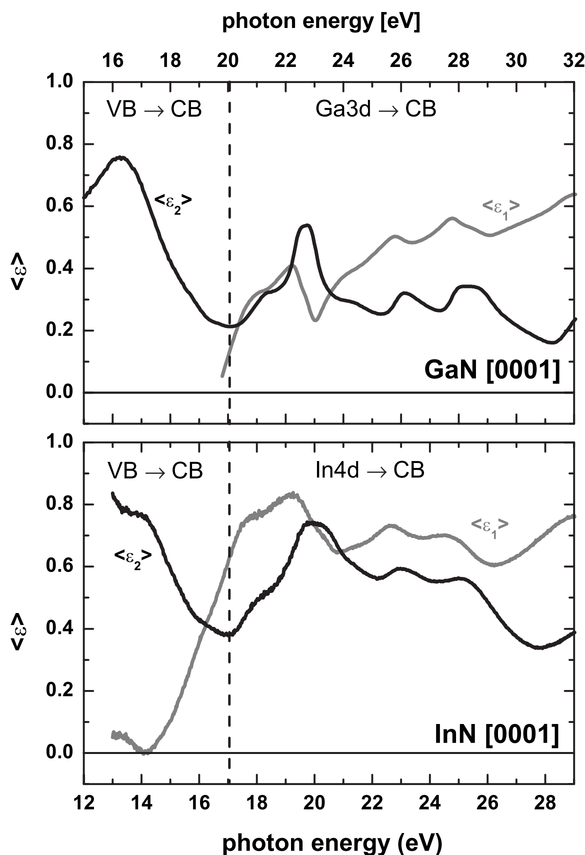

FIG. 2. Real (gray) and imaginary (black) parts of the ordinary DF $\varepsilon^{\perp}$ measured on wurtzite GaN and InN. For comparison, the GaN DF is plotted in the upper graph between 15 and 32 eV, while the InN DF is drawn in the lower graph between 12 and 29 eV.

V. RESULTS AND DISCUSSION

The wurtzite DF was measured first on *c*-plane [0001] GaN and InN films. Figure 2 shows the real and imaginary parts of the effective DF for both in the spectral range of *d*-level excitations. These effective DFs measured on [0001] films represent the ordinary components $\varepsilon^{\perp}$ related to an electric field perpendicular to the *c* axis. Both spectra contain residual interband transition structures below 20 and 17 eV, respectively. The magnitude of all higher energy peaks above the plasma edge does not exceed an amplitude of 1 in $\langle \varepsilon_2 \rangle$. The constituting electronic transitions are basically Ga 3*d* (In 4*d*) core level excitations to conduction-band states. Thus, the DF in this spectral range is proportional to the number of excited electrons and should be directly related to the *p*-orbital projected partial density of conduction-band states (*p*-PDOS) perpendicular to the *c* axis [see relation (3)].

It is remarkable that the observed DF line shapes for both materials closely resemble each other apart from an overall energy shift and a constant scaling factor. This indicates a very similar conduction-band *p*-PDOS in wurtzite GaN and InN. The similarities in the DFs are in sharp contrast to the results obtained at lower photon energies, where the respective DFs are conspicuously different, i.e., material specific.[2,3,19]

Absorption features in this lower photon energy range correlate to the combined density of states of both valence and conduction band at high symmetry points or lines in the Brillouin zone. If the conduction bands of InN and GaN are assumed to be very similar, differences among the interband transitions must relate exclusively to a different dispersion and wave function character of the valence band in GaN and InN.

In the core level excitation regime, the observed rigid energy shift of excitation features in GaN with respect to InN amounts to 2.5–3 eV. XPS measurements on InGaP (Ref. 35) and InGaN,[36] on the other hand, show a binding energy difference of about 1.8–2.0 eV between the Ga 3*d* and In 4*d* electronic states. Thus, the observed energy shift in the DF relates to a large amount to the different binding energies of the initial *d* states. We attribute the remaining shift of about 0.5–1 eV to a different energy of the lowest *p*-like conduction bands. For the latter conclusion, we have presumed identical exciton related energy shifts for the GaN and InN *d* level excitation.

In InN, the first *d*-level transition to a *p*-like conduction band appears at ≈18.0 eV, while in GaN, the first transition is observed at ≈21.3 eV. For comparison, recent photoemission experiments of Piper *et al.*[5] revealed the In $4d_{5/2}$ electrons in InN 16.0 ± 0.1 eV below the valence band maximum. The Ga 3*d* electron binding energy in GaN was determined by Lambrecht *et al.*[12] to be 17.1 ± 0.1 eV with respect to the valence band maximum. Furthermore, the band gaps of both materials are ≈0.7 and ≈3.4 eV, respectively. In combination, these results would indicate that the lowest *p*-like conduction bands are located just about 1 eV above the conduction-band minimum. Nevertheless, we assume these bands at a considerable higher position. It is known that quasiparticle and excitonic effects introduce an energy offset. For example, Aspnes *et al.* have determined an exciton binding energy of 0.66 eV for In 4*d* transition in InAs.[4] Furthermore, there are discrepancies in the reported photoemission experiments and it is not clear whether the determined absolute binding energies are correct. The binding energy difference between the In 4*d* and Ga 3*d* levels in InGaP or InGaN (1.8–2.0 eV) is obviously different to those deduced from the measurements on InN and GaN (1.1 eV).

A closer examination of the presented core level excitation spectra reveals a double-peak structure of all Ga 3*d* (In 4*d*) related transition features. These double peaks originate from a splitting of the semicore *d* level induced by the spin-orbit interaction and crystal field effects. In room temperature spectra, this splitting is apparent only for the strongest transition structures. The most accurate method for determining the transition energies is the analysis of the derivatives of the DF.[37] Similar to our previous studies of the Van Hove singularities[38] below 10 eV, the third derivative is employed in the current studies in order to separate small features. Figure 3 shows the corresponding spectra in the region of the first and second *d*-level related peak, as obtained from the low-temperature DF. In this representation, both transitions clearly break into two components. The splitting was additionally proven by fitting the spectra with pairs of Lorentz oscillators. We obtain a spin-orbit separation of Δd=0.41 ± 0.01 eV for GaN and Δd=0.82 ± 0.01 eV for

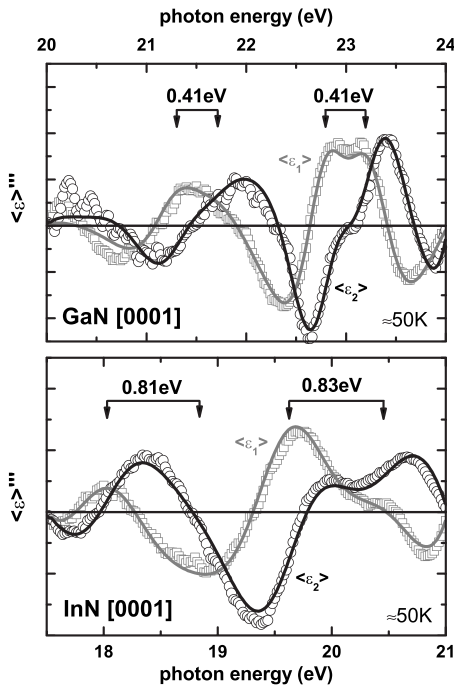

FIG. 3. Third derivative of $\langle \varepsilon^{\perp} \rangle$ of GaN (upper graph) and InN (lower graph) around the two dominant core level excitation peaks. The spin-orbit splitting of the Ga 3*d* and In 4*d* levels is labeled with arrows. Applying a Lorentz-oscillator fit (solid curve), we deduce a spin-orbit separation of 0.41 and 0.82 ± 0.01 eV, respectively.

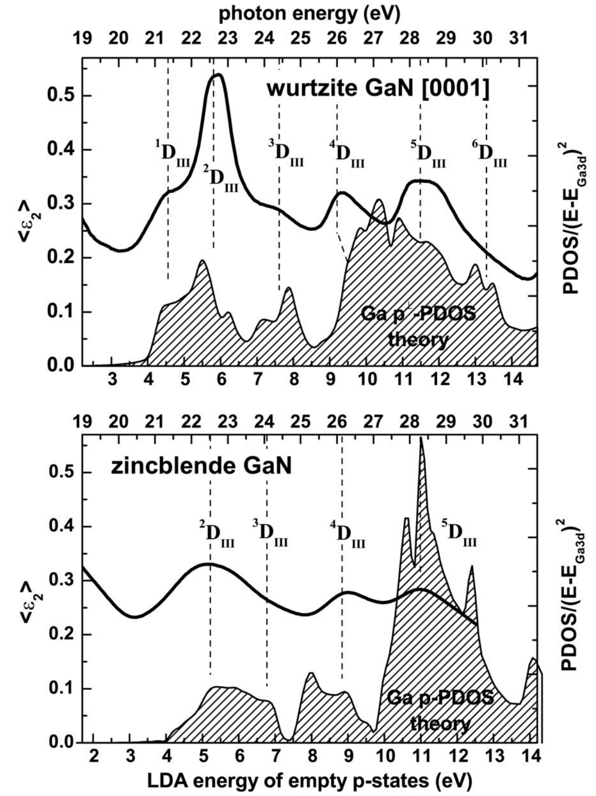

FIG. 4. The upper graph shows the imaginary part of the wurtzite GaN DF in comparison with the calculated PDOS of the *p*-like empty states in the [0001] plane and around the Ga atoms (patterned). In the lower graph, the same comparison is shown for zinc blende GaN. In both cases, the top scale indicates the photon energy range of the ellipsometric measurement, while the bottom scale indicates calculated conduction-band energies corresponding to the energy scale in Fig. 5.

InN, which is in agreement with former measurements.[4,39]

In the upper part of Fig. 4, we compare, for wurtzite GaN, the measured ordinary DF $\varepsilon^{\perp}$ with the calculated PDOS of *p*-like conduction-band states from the [0001] plane (Ga site). In fact, the DF structures are fairly reproduced by the calculated PDOS, although excitonic effects[4] as well as *k* and energy dependent variations of the matrix elements P_{cv} can influence the line shape and relative amplitudes in the DF [see relation (1)]. In particular, the strong transfer of transition oscillator strength from higher to lower photon energies is well known and analyzed, e.g., for the interband transition regime.[28,40] However, the experimental spectra exhibit six major transition structures, which are reproduced by similar peaks in the PDOS. These structures are denoted by $^1D_{III}$-$^6D_{III}$ according to the notation of Cardona *et al.* in Ref. 41. The index number is a running count of transitions, while the term D_{III} points out that the initial states are *d* states of the group III metal.

A possible correlation of peaks in the PDOS (DF) to certain conduction-band areas is demonstrated in Fig. 5. According to this comparison between the band structure and PDOS, the $^1D_{III}$ transition relates to a nondispersive conduction-band branch between the Γ and the *A* point at ≈4 eV. Furthermore, we would attribute $^3D_{III}$ and $^4D_{III}$ to conduction-band states near the *L* point of the wurtzite Brillouin zone. However, at higher photon energies, such an assignment becomes more arguable due to the complexity of the wurtzite band structure. However, all higher conduction-band states have a dominant *p*-orbital symmetry and therefore contribute to the dielectric function in this energy range. Only the lowest conduction-band states have an increasing *s*-symmetry fraction. An excitation of *d* electrons to the conduction-band minimum is therefore not allowed.

In the lower part of Fig. 4, we compare the measured DF with the calculated PDOS of *p*-like conduction-band states (Ga site) for zinc blende GaN. The integrated density of conduction-band states was assumed to be similar for both crystal structures. This is, in fact, reproduced in our ellipsometric measurements on wurtzite and zinc blende GaN. The lower overall amplitude and the broadening of transition features in the zinc blende DF is mainly related to the lower crystal quality in comparison with the wurtzite sample. The essential difference between the wurtzite and zinc blende DF (PDOS) is the absence of the $^1D_{III}$ structure in the zinc blende case. We have attributed the $^1D_{III}$ structure to dispersionless conduction-band states between the Γ and the *A* point in the wurtzite Brillouin zone. These wurtzite states emerge due to the back folding of the lowest cubic conduction band in the Γ-*L* direction.[42,43] Consequently, the $^1D_{III}$ structure does not appear in the zinc blende phase.

On the other hand, we have attributed the $^3D_{III}$ and $^4D_{III}$ structures, e.g., to nondispersive conduction-band states along the wurtzite *M*-*L* line. This symmetry line includes the prominent point at 2/3*M*-*L*, which refers to the $L_{\perp}$ point in

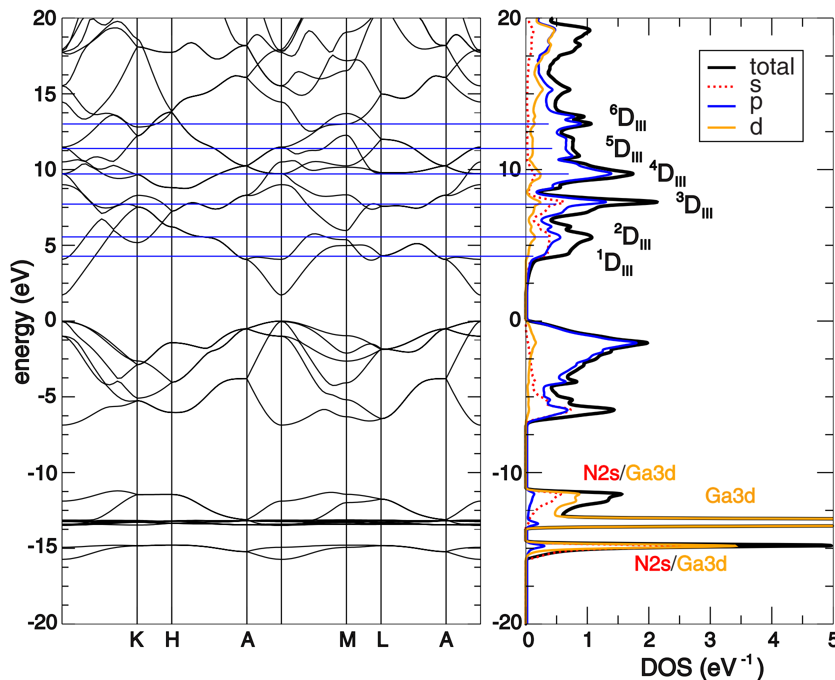

FIG. 5. (Color online) DFT-LDA band structure calculation (left) of wurtzite GaN and the deduced DOS (right). The DOS is shown in components with *s*, *p*, and *d* symmetries. An assignment of structures $^1D_{III}$-$^5D_{III}$ to conduction-band states is indicated by horizontal lines. Notice that the peak maximum of the Ga 3*d* DOS is much larger than the shown DOS range.

the respective zinc blende Brillouin zone. Accordingly, these features occur in both crystal modifications and relate to the lowest zinc blende conduction bands around the $L_\perp$ point. Finally, we attribute the dominant $^2D_{III}$ structure to the lowest conduction-band states at the zinc blende X point.[4]

Figure 6 shows the comparison of the measured ordinary DF $\varepsilon^\perp$ and the calculated PDOS of *p*-like states (In site) for wurtzite InN. Like in GaN, we find an agreement of absorption structures in the imaginary part of the DF with respective maxima in the PDOS. The amplitude of the first transition features in the DF, however, is again exaggerated most likely due to the strong influence of excitonic effects. At higher energies, the calculated PDOS of InN differs from the GaN PDOS, although the measured DF is quite similar in line shape. Furthermore, all characteristic maxima in the InN PDOS are predicted at about 1 eV lower energies than in GaN. This is in very good agreement with the experimental results if we assume that the binding energy of the In 4*d* electrons in InN is 2 eV smaller than the binding energy of the Ga 3*d* electrons in GaN.

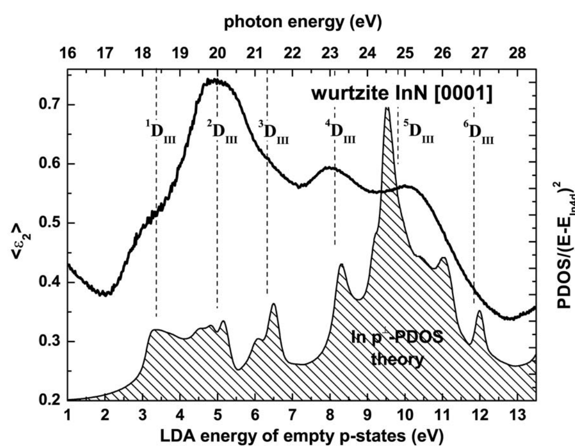

FIG. 6. Imaginary part of the wurtzite InN DF in comparison with the calculated PDOS of the *p*-like empty states in the [0001] plane and around the In atoms (patterned). The top scale indicates the photon energy range of the ellipsometric measurement, while the bottom scale indicates the conduction-band energies, as calculated in the DFT-LDA.

By measuring *M*-plane GaN $(1\bar{1}00)$ and *a*-plane InN $(11\bar{2}0)$, respectively, with the *c* axis either parallel or perpendicularly oriented to the plane of incidence, we determined both the ordinary $\varepsilon^\perp$ and the extraordinary $\varepsilon^\parallel$ dielectric tensor components (Fig. 7). The reduced overall amplitudes, the broadening of structures, and the poor signal to noise ratio are again a consequence of the lower crystal quality and higher surface roughness of these samples, as compared to the respective *c*-plane materials. Nevertheless, we resolve differences in the extraordinary component, while the ordinary component, as expected, agrees with the results obtained on the *c*-plane samples. Furthermore, we can also confirm good agreement of the respective calculated PDOS components with the measured dielectric tensor components, although momentum matrix elements again are not taken into account. Our ellipsometric measurements as well as the DFT-LDA calculations show for the components parallel to the *c* axis an increased amplitude of the $^3D_{III}$, $^4D_{III}$, and $^6D_{III}$ structures, while $^1D_{III}$, $^2D_{III}$, and, in particular, $^5D_{III}$ are smaller (Fig. 7). This DOS transfer demonstrates a direction dependent mixing of the empty *p* states. In contrast to polarization dependent x-ray absorption measurements,[31] we found no evidence for a reasonable energy shift of GaN PDOS maxima either in the *ab initio* calculations or in the ellipsometric results. In other words, the PDOS anisotropy arises from variations in PDOS amplitudes but not from an energy shift of electronic bands.

Only the $^2D_{III}$ structure in the InN DF and PDOS, respectively, reveals a small energy shift in theory and experiment.

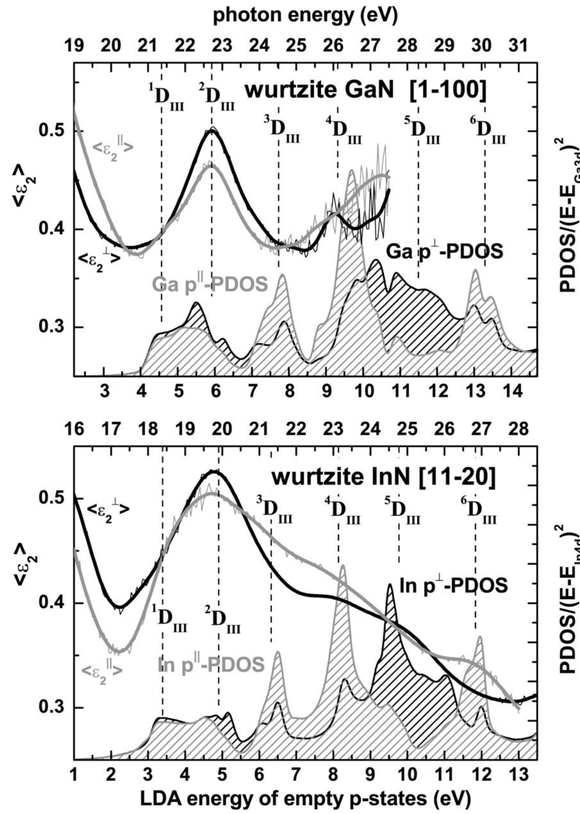

FIG. 7. Anisotropy of the PDOS in p-like empty states and the respective imaginary part of the DF measured on wurtzite GaN$[1\bar{1}00]$ (upper graph) and wurtzite InN$[11\bar{2}0]$ (lower graph). The PDOS was calculated by DFT-LDA. The black lines denote the the ordinary components perpendicular to the $[0001]$ c axis, and the gray lines the extraordinary component parallel to the $[0001]$ c axis. In both cases, the top scale indicates the photon energy range of the ellipsometric measurements, while the bottom scale indicates calculated conduction-band energies corresponding to the energy scale like in Fig. 5.

This shift can be explained by a distortion (bending) of the chemical bonds along the c axis (π bonds) with respect to bonds in the c plane (σ bonds), as suggested in Ref. 31. Such a distortion is governed by the c/a ratio or internal bond-length parameter u. The latter determines the position of the anion relative to the cation sublattice. In the "ideal" case, these parameters are $u_{ideal}=3/8=0.375$ and $c/a_{ideal}=\sqrt{8/3}=1.633$. Any deviation might be an indicator for noncubic crystal field and additional deformation (anisotropy) in the chemical tetragonal bonding, respectively.[44] In our *ab initio* calculation for InN (Fig. 7), we have obtained after optimization of ion positions $u=0.379$ and $c/a=1.630$. However, these values are much closer to the ideal values than that measured on our a-plane InN sample ($c/a_{expt}=1.613$) (Ref. 38) or those published by Kim *et al.*[45] ($u_{theor}=0.388$) and Davydov *et al.*[46] ($c/a_{expt}=1.613$). For GaN, it is known that the intrinsic deformation of chemical bonding is small. Accordingly, the calculated value for u_{GaN} is 0.377, very close to the ideal value of a wurtzite crystal. Thus, a reasonable shift of electronic states in the two directions is unlikely. Lattice parameter deviations measured by XRD in our M-plane GaN sample are mostly induced by tensile strain parallel and compressive strain perpendicular to the growth direction.[21]

VI. CONCLUSIONS

Spectroscopic ellipsometry was used in the spectral range of metal d-level excitations to the lower p-like empty states (16–30 eV) in order to probe the conduction-band DOS on the metal sites in InN and GaN. The measured dielectric function is assumed to be proportional to the to p-like DOS. This is proven by a comparison to direction dependent DOS calculations within DFT-LDA. Our measurements show a high conformity of the wurtzite InN and GaN p-like conduction-band DOSs perpendicular to the crystal axis (perpendicular to the c axis). However, respective peaks in the DOS of InN appear shifted by about 2.5–3 eV to lower energies in comparison with GaN. On the basis of the DFT-LDA band structure calculations, pronounced maxima in the dielectric function and DOS, respectively, were assigned to certain points or lines in the Brillouin zone. A comparison of wurtzite and zinc blende GaN further shows a high overall agreement of the p-like conduction-band DOS in the hexagonal and cubic crystal modification. Specific additional maxima in the wurtzite GaN DOS are, for example, explained by a back folding of conduction bands in the smaller wurtzite Brillouin zone. Ellipsometric measurements on wurtzite samples with the c axis in the surface plane and direction dependent DFT-LDA calculations were also used to study anisotropies in the conduction-band DOS. We found a distinct anisotropy in the amplitude of DOS maxima and the respective dielectric functions, while the energy of p-like conduction bands is almost identical. The fine structure in all absorption features measured by ellipsometry is attributed to the spin orbit splitting of the In $4d$ and Ga $3d$ levels. By analyzing the dielectric function in the third derivative, the spin-orbit splitting is determined to be 0.82 and 0.41 eV (± 0.01 eV) for InN and GaN, respectively.

ACKNOWLEDGMENTS

The authors would like to thank O. Brandt (Paul Drude Institute for Solid State Electronics, Berlin, Germany) as well as D. J. As, D. Schikora, and K. Lischka (Universität Paderborn, Germany) for the support with GaN samples. Furthermore, the authors gratefully acknowledge the support of the BESSY GmbH and co-workers. This work was financially supported by the Bundesministerium für Bildung und Forschung (BMBF) under the Contract NOs. 05 KS4KTB/3 and 05ES3XBA/5.

*Present address: Paul-Drude-Institut, 10117 Berlin, Germany.
†chrcobet@isas.de

[1] R. Goldhahn, C. Buchheim, P. Schley, A. T. Winzer, and H. Wenzel, in *Nitride Semiconductor Devices: Principles and Simulation*, edited by J. Piprek (Wiley, Weinheim, 2007), p. 95.
[2] C. Cobet *et al.*, Phys. Rev. B **64**, 165203 (2001).
[3] R. Goldhahn, A. T. Winzer, V. Cimalla, O. Ambacher, C. Cobet, W. Richter, N. Esser, J. Furthmüller, F. Bechstedt, H. Lu, and W. J. Schaff, Superlattices Microstruct. **36**, 591 (2004).
[4] D. E. Aspnes, M. Cardona, V. Saile, M. Skibowski, and G. Sprüssel, Solid State Commun. **31**, 99 (1979).
[5] L. F. J. Piper, T. D. Veal, P. H. Jefferson, C. F. McConville, F. Fuchs, J. Furthmüller, F. Bechstedt, H. Lu, and W. J. Schaff, Phys. Rev. B **72**, 245319 (2005).
[6] S. A. Ding, G. Neuhold, J. H. Weaver, P. Häerle, K. Horn, O. Brandt, H. Yang, and K. Ploog, J. Vac. Sci. Technol. A **14**, 819 (1996).
[7] C. Persson and A. Zunger, Phys. Rev. B **68**, 073205 (2003).
[8] D. Fritsch, H. Schmidt, and M. Grundmann, Phys. Rev. B **67**, 235205 (2003).
[9] L. E. Ramos, L. K. Teles, L. M. R. Scolfaro, J. L. P. Castineira, A. L. Rosa, and J. R. Leite, Phys. Rev. B **63**, 165210 (2001).
[10] Y.-N. Xu and W. Y. Ching, Phys. Rev. B **48**, 4335 (1993).
[11] J. Furthmüller, P. H. Hahn, F. Fuchs, and F. Bechstedt, Phys. Rev. B **72**, 205106 (2005).
[12] W. R. L. Lambrecht, B. Segall, S. Strite, G. Martin, A. Agarwal, H. Morkoc, and A. Rockett, Phys. Rev. B **50**, 14155 (1994).
[13] W. R. L. Lambrecht, B. Segall, J. Rife, W. R. Hunter, and D. K. Wickenden, Phys. Rev. B **51**, 13516 (1995).
[14] C. B. Stagarescu, L.-C. Duda, K. E. Smith, J. H. Guo, J. Nordgren, R. Singh, and T. D. Moustakas, Phys. Rev. B **54**, R17335 (1996).
[15] B. Bouhafs, F. Litimein, Z. Dridi, and P. Ruterana, Phys. Status Solidi B **236**, 61 (2003).
[16] F. Litimein, B. Bouhafs, and P. Ruterana, Phys. Status Solidi A **203**, 35 (2006).
[17] R. L. Johnson, J. Barth, M. Cardona, D. Fuchs, and A. M. Bradshaw, Nucl. Instrum. Methods Phys. Res. A **290**, 606 (1990).
[18] H. G. Tompkins and E. A. Irene, *Handbook of Ellipsometry* (William Andrew, Norwich, 2005).
[19] L. X. Benedict, T. Wethkamp, K. Wilmers, C. Cobet, N. Esser, E. L. Shirley, W. Richter, and M. Cardona, Solid State Commun. **112**, 129 (1999).
[20] P. Waltereit, O. Brandt, M. Ramsteiner, A. Trampert, H. T. Grahn, J. Menniger, M. Reiche, and K. H. Ploog, J. Cryst. Growth **227-228**, 437 (2001).
[21] P. Waltereit, O. Brandt, M. Ramsteiner, R. Uecker, P. Reiche, and K. H. Ploog, J. Cryst. Growth **218**, 143 (2000).
[22] D. J. As, D. Schikora, and K. Lischka, Phys. Status Solidi C **0**, 1607 (2003).
[23] H. Lu, W. J. Schaff, L. F. Eastman, J. Wu, W. Walukiewicz, V. Cimalla, and O. Ambacher, Appl. Phys. Lett. **83**, 1136 (2003).
[24] R. Goldhahn, P. Schley, A. T. Winzer, M. Rakel, C. Cobet, N. Esser, H. Lu, and W. J. Schaff, J. Cryst. Growth **288**, 273 (2006).
[25] H. Ehrenreich and M. H. Cohen, Phys. Rev. **115**, 786 (1959).
[26] S. L. Adler, Phys. Rev. **126**, 413 (1962).
[27] N. Wiser, Phys. Rev. **129**, 62 (1963).
[28] P. Y. Yu and M. Cardona, *Fundamentals of Semiconductors* (Springer-Verlag, Berlin, 1996).
[29] D. E. Aspnes, in *Handbook On Semiconductors*, edited by T. S. Moss (North-Holland, Amsterdam, 1980), Vol. II, pp. 109–154.
[30] P. Lautenschlager, P. B. Allen, and M. Cardona, Phys. Rev. B **33**, 5501 (1986).
[31] K. Lawniczak-Jablonska, T. Suski, I. Gorczyca, N. E. Christensen, K. E. Attenkofer, R. C. C. Perera, E. M. Gullikson, J. H. Underwood, D. L. Ederer, and Z. Liliental Weber, Phys. Rev. B **61**, 16623 (2000).
[32] G. Kresse and J. Furthmüller, Phys. Rev. B **54**, 11169 (1996).
[33] G. Kresse and D. Joubert, Phys. Rev. B **59**, 1758 (1999).
[34] P. E. Blöchl, O. Jepsen, and O. K. Andersen, Phys. Rev. B **49**, 16223 (1994).
[35] P. Vogt, K. Lüdge, M. Zorn, M. Pristovsek, W. Braun, W. Richter, and N. Esser, Phys. Rev. B **62**, 12601 (2000).
[36] J. E. Downes, K. E. Smith, A. Y. Matsuurab, I. Lindau, E. Iliopoulos, and T. D. Moustakas, J. Appl. Phys. **94**, 5820 (2003).
[37] D. E. Aspnes, Phys. Rev. Lett. **28**, 168 (1972).
[38] P. Schley, R. Goldhahn, A. T. Winzer, G. Gobsch, V. Cimalla, O. Ambacher, H. Lu, W. J. Schaff, M. Kurouchi, Y. Nanishi, M. Rakel, C. Cobet, and N. Esser, Phys. Rev. B **75**, 205204 (2007).
[39] C. G. Olson, D. W. Lynch, and A. Zehe, Phys. Rev. B **24**, 4629 (1981).
[40] L. X. Benedict and E. L. Shirley, Phys. Rev. B **59**, 5441 (1999).
[41] M. Cardona, W. Gudat, E. E. Koch, M. Skibowski, B. Sonntag, and P. Y. Yu, Phys. Rev. Lett. **25**, 659 (1970).
[42] J. L. Birman, Phys. Rev. **115**, 1493 (1959).
[43] M. Cardona and G. Haberke, Phys. Rev. **137**, 1467 (1965).
[44] N. E. Christensen and I. Gorczyca, Phys. Rev. B **47**, 4307 (1993).
[45] K. Kim, W. R. L. Lambrecht, and B. Segall, Phys. Rev. B **53**, 16310 (1996).
[46] V. Y. Davydov *et al.*, Phys. Status Solidi B **229**, R1 (2002).